Observer Based Method for Joint Torque Estimation in Active Orthoses ⋆

Markus Grün * **Ulrich Konigorski** **

* *Department of Control Engineering and Mechatronics, Technische Universität Darmstadt, Darmstadt, Germany (e-mail: mgruen@iat.tu-darmstadt.de).*
** *Department of Control Engineering and Mechatronics, Technische Universität Darmstadt, Darmstadt, Germany (e-mail: ukonigorski@iat.tu-darmstadt.de).*

Abstract: This contribution presents a new approach of estimating the joint torques for an active orthosis. The new approach combines inverse dynamics and measured ground reaction forces. The joint torques can easily be computed from the ground reaction forces, but the measurement is usually flawed. An obsererver is employed to estimate the disturbance of the measurements and restore the original joint torques.
A model of the human lower extremity is presented and additional seat forces are introduced to model the seat. Simulation results on the Sit-to-Stand movement illustrate the effectivity of the new approach.

Keywords: Exoskeleton, Active Orthosis, Observer, Joint Torque, Ground Reaction Forces

1. INTRODUCTION

Active orthoses and motorized exoskeletons are subject to numerous research projects. The objectives of these projects are manifold and reach from tremor suppression, rehabilitation for several limbs after stroke or injury, to strength enhancing of the lower extremities or the hole body.

The active orthosis currently under development at our research group is an exoskeleton for the lower limbs with a motorized knee joint. The orthosis is designed to support elderly people or people with disabilities with an additional torque at the knee joint during challenging tasks like the Sit-To-Stand movement (STS) or climbing stairs, for example.

For orthoses that enhance the user's strength or reduce the user's effort for a given task, several controllers have been proposed in the literature, see Pratt et al. (2004), Kong and Tomizuka (2009), Fleischer and Hommel (2006), for example. The reference input to these controllers is the joint torque that the user applies to his body. By amplifying the joint torque, the user's strength can be enhanced or the effort can be reduced.

A reliable measurement or estimate of the user's joint torques is therefore essential and plays a major role in the control system. Three methods have proven their effectiveness:

Electromyography (EMG) Using several electrodes applied to the skin, the activity of the underlying muscle can be measured. Deriving a feasible value for the force this muscle generates, however, is difficult and subject to many disturbances. This method also requires extensive preparation during putting on and taking off of the orthosis. It is used by the exoskeleton HAL (Hayashi et al. (2005)), or Fleischer and Hommel (2006), for example.

Inverse Dynamics The joint torques can be calculated using an inverse model of the human lower extremity. High resolution and low noise angular sensors are required since the angular value needs to be differentiated twice. Furthermore, the computed joint torques strongly depend on the accuracy of the model. A little error in the model causes large deviations in the joint torques. During gait, the inverse dynamics need to be switched between different models. The Berkeley Lower Extremity Exoskeleton (BLEEX, Kazerooni et al. (2005)) or Kong and Tomizuka (2009), for example, use inverse dynamics to compute the joint torques.

Ground Reaction Forces (GRF) The contact force between the foot and the ground, and the center of pressure (CoP) can be measured using force sensors in the shoe sole. The ankle joint torque can be directly calculated from these values, and with an angular sensor at the ankle joint, the knee torque can be calculated as well. However, the computed joint torques strongly depend on the correct measurement of the CoP. Also, the shear force must be measured for an exact calculation of the joint torques. The RoboKnee (Pratt et al. (2004)) uses this method for example, though the ankle angle is not measured.

In this paper, an alternative approach is proposed which combines inverse dynamics and the calculation of the joint torques using ground reaction forces. An observer estimates the error in the joint torque calculation and

⋆ The authors gratefully thank the Deutsche Forschungsgemeinschaft (DFG) for funding this work by the project with the reference number KO 1876/12-1

adjusts the result. A model of the human lower extremity will be introduced and simulation results will be shown for the Sit-to-Stand transfer. The performance of the new approach will be compared to the results of using only inverse dynamics and using only ground reaction forces, respectively.

2. MODELLING

This section describes the modelling of the human lower extremity. This model will be used for calculating the simulations results presented in section 5.

2.1 Model of Human Lower Extremity

It is assumed that movement is only in the saggital plane of the human body and that the movement of the right and left leg are symmetric. To further simplify the model, the upper body is modeled as a single mass. This allows modelling the lower extremities as a two link chain or double inverted pendulum, which is fixed at the ground. The seat is modeled as external forces $F_{\mathrm{Seat,h}}$ and $F_{\mathrm{Seat,v}}$ that act on the inverted pendulum as seen in Fig. 1. These forces prevent the pendulum from collapsing in the sitting position.

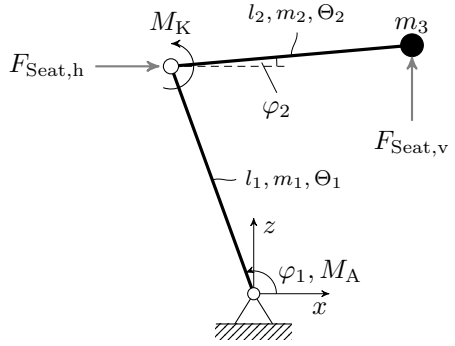

Fig. 1. Model of human lower extremity in sitting position

The seat forces are only active within a limited position of the pendulum and cease after the Seat-Off. The specifications of the seat forces will be given in section 2.3. But first, the equations of motion of the double inverted pendulum are derived by Lagrangian mechanics.

The kinematic equations describe the movement of the centers of mass of the two rigid beams and the body mass m_3:

$$\mathbf{s_1} = \begin{bmatrix} s_{1,x} \\ s_{1,z} \end{bmatrix} = \begin{bmatrix} \frac{l_1}{2}\cos(\varphi_1) \\ \frac{l_1}{2}\sin(\varphi_1) \end{bmatrix}$$

$$\mathbf{s_2} = \begin{bmatrix} s_{2,x} \\ s_{2,z} \end{bmatrix} = \begin{bmatrix} l_1\cos(\varphi_1) + \frac{l_2}{2}\cos(\varphi_2) \\ l_1\sin(\varphi_1) + \frac{l_2}{2}\sin(\varphi_2) \end{bmatrix} \tag{1}$$

$$\mathbf{s_3} = \begin{bmatrix} s_{3,x} \\ s_{3,z} \end{bmatrix} = \begin{bmatrix} l_1\cos(\varphi_1) + l_2\cos(\varphi_2) \\ l_1\sin(\varphi_1) + l_2\sin(\varphi_2) \end{bmatrix}.$$

The time dependencies of the coordinate functions are omitted for simplicity. The velocities follow by time differentiation of (1):

$$\mathbf{v_1} = \frac{\mathrm{d}}{\mathrm{d}t}\mathbf{s_1}, \quad \mathbf{v_2} = \frac{\mathrm{d}}{\mathrm{d}t}\mathbf{s_2}, \quad \mathbf{v_3} = \frac{\mathrm{d}}{\mathrm{d}t}\mathbf{s_3}. \tag{2}$$

With the angular velocities ω_1 and ω_2 at the two joints and (2) the kinetic energies can be calculated:

$$\begin{aligned} E_{\mathrm{kin},1} &= \tfrac{1}{2}\Theta_1\omega_1^2 \\ E_{\mathrm{kin},2} &= \tfrac{1}{2}\Theta_2\omega_2^2 + \tfrac{1}{2}m_2{\mathbf{v_2}}^2 \\ E_{\mathrm{kin},3} &= \tfrac{1}{2}m_3{\mathbf{v_3}}^2. \end{aligned} \tag{3}$$

The potential energies are calculated with the z-components of (1)

$$\begin{aligned} E_{\mathrm{pot},1} &= m_1\, g\, s_{1,z} \\ E_{\mathrm{pot},2} &= m_2\, g\, s_{2,z} \\ E_{\mathrm{pot},3} &= m_3\, g\, s_{3,z} \end{aligned} \tag{4}$$

and with (3) and (4) the Lagrangian function becomes

$$L = \sum_{i=1}^{3} \left(E_{\mathrm{kin},i} - E_{\mathrm{pot},i}\right). \tag{5}$$

The work of the seat forces and the friction is defined as follows:

$$\begin{aligned} W_{\mathrm{d}} &= d_1\omega_1\varphi_1 + d_2(\omega_2 - \omega_1)(\varphi_2 - \varphi_1) \\ W_{\mathrm{Seat}} &= F_{\mathrm{Seat,v}}\, s_{3,z} + F_{\mathrm{Seat,h}} \sin\left(\varphi_1 - \tfrac{\pi}{2}\right) l_1. \end{aligned} \tag{6}$$

With the work of the knee and ankle torque

$$W_{\mathrm{u}} = M_{\mathrm{A}}\varphi_1 + M_{\mathrm{K}}\left(\varphi_2 - \varphi_1\right) \tag{7}$$

the overall work can be expressed

$$Q = W_{\mathrm{u}} + W_{\mathrm{Seat}} - W_{\mathrm{d}} \tag{8}$$

and the equations of motion can now be computed using the well known Lagrange's equation

$$\frac{\mathrm{d}}{\mathrm{d}t}\left(\frac{\partial L}{\partial \dot{\mathbf{q}}}\right) - \frac{\partial L}{\partial \mathbf{q}} = Q. \tag{9}$$

The left side of the above equation corresponds to the left side of the nonlinear function of equations of motion

$$\mathbf{M}(\mathbf{q})\ddot{\mathbf{q}} + \mathbf{K}(\mathbf{q},\dot{\mathbf{q}}) = \mathbf{F}_{\mathrm{u}}(\mathbf{q},\dot{\mathbf{q}})\mathbf{u} + \mathbf{F}_{\mathrm{f}}(\mathbf{q},\dot{\mathbf{q}})\mathbf{f}_{\mathrm{Seat}} \tag{10}$$

except for the terms containing the friction d. $\mathbf{q}$ is $[\varphi_1 \;\; \varphi_2]^{\mathrm{T}}$, $\mathbf{u}$ is $[M_{\mathrm{A}} \;\; M_{\mathrm{K}}]^{\mathrm{T}}$, and $\mathbf{f}_{\mathrm{Seat}}$ is $[F_{\mathrm{Seat,v}} \;\; F_{\mathrm{Seat,h}}]^{\mathrm{T}}$.

The matrix $\mathbf{M}$ can be obtained by differentiating the left side of (9) with respect to $\ddot{\mathbf{q}}$:

$$\mathbf{M} = \frac{\partial}{\partial \ddot{\mathbf{q}}}\left[\frac{\mathrm{d}}{\mathrm{d}t}\left(\frac{\partial L}{\partial \dot{\mathbf{q}}}\right) - \frac{\partial L}{\partial \mathbf{q}}\right]. \tag{11}$$

The input matrices $\mathbf{F}_{\mathrm{u}}$ and $\mathbf{F}_{\mathrm{f}}$ can be obtained in a similar way:

$$\mathbf{F}_{\mathrm{u}} = \frac{\partial Q}{\partial \mathbf{u}}, \quad \mathbf{F}_{\mathrm{f}} = \frac{\partial Q}{\partial \mathbf{f}_{\mathrm{Seat}}} \tag{12}$$

and $\mathbf{K}$ results from:

$$\mathbf{K} = \frac{\mathrm{d}}{\mathrm{d}t}\left(\frac{\partial L}{\partial \dot{\mathbf{q}}}\right) - \frac{\partial L}{\partial \mathbf{q}} - \mathbf{M}\ddot{\mathbf{q}} + \frac{\partial}{\partial \mathbf{q}}W_{\mathrm{d}}. \tag{13}$$

The nonlinear state space description

$$\begin{aligned} \dot{\mathbf{x}} &= \mathbf{f}(\mathbf{x}) + \mathbf{g}_{\mathrm{u}}(\mathbf{x})\mathbf{u} + \mathbf{g}_{\mathrm{f}}(\mathbf{x})\mathbf{f}_{\mathrm{Seat}} \\ \mathbf{y} &= \mathbf{h}(\mathbf{x}) \end{aligned} \tag{14}$$

finally follows with (11) – (13)

$$\begin{bmatrix} \dot{\mathbf{q}} \\ \ddot{\mathbf{q}} \end{bmatrix} = \begin{bmatrix} \dot{\mathbf{q}} \\ -\mathbf{M}^{-1}\,\mathbf{K} \end{bmatrix} + \begin{bmatrix} \mathbf{0} \\ -\mathbf{M}^{-1}\,\mathbf{F}_{\mathrm{u}} \end{bmatrix}\mathbf{u} + \begin{bmatrix} \mathbf{0} \\ -\mathbf{M}^{-1}\,\mathbf{F}_{\mathrm{f}} \end{bmatrix}\mathbf{f}_{\mathrm{Seat}} \tag{15}$$

2.2 Superior Controller

For the system (15) presented above, a decoupling controller can be derived using *exact linearization* as described in Isidori (1995), for example. This controller represents the "human brain" and provides an appropriate input $\mathbf{u}$ to move the model from the sitting position to the standing position. The derivation of the controller is straight forward as the sum of the relative degrees δ_i equals the order of the system n; hence, no zero dynamics are present.

Simulation results shown in this paper are calculated using this controller; however, a detailed description is omitted as it is not relevant for the proposed approach of computing the joint torques.

2.3 Seat Forces

All joint torques should be zero in the sitting position. The additional seat forces introduced in section 2.1 are dimensioned such that this demand is met and that they fade after a certain height h_{SO}. This moment is called "Seat-Off" and describes the point where the body leaves the seat and all muscles have to carry the full body weight.

To fulfill these requirements, the seat forces are defined as follows. The corresponding parameters are depicted in Fig. 2.

$$F_{\mathrm{Seat,v}} = \begin{cases} c_{\mathrm{v}} \left(s_{3,z} - h_{\mathrm{SO}}\right)^2, & \text{for } s_{3,z} < h_{\mathrm{SO}} \\ 0, & \text{for } s_{3,z} \geq h_{\mathrm{SO}} \end{cases} \tag{16}$$

$$F_{\mathrm{Seat,h}} = \begin{cases} c_{\mathrm{h}} \left(s_{3,z} - h_{\mathrm{SO}}\right)^2, & \text{for } s_{3,z} < h_{\mathrm{SO}} \\ 0, & \text{for } s_{3,z} \geq h_{\mathrm{SO}} \end{cases} \tag{17}$$

with

$$c_{\mathrm{v}} = \frac{\left(\frac{1}{2}m_2 + m_3\right) g}{\left(z_{3,0} - h_{\mathrm{SO}}\right)^2} \tag{18}$$

$$c_{\mathrm{h}} = \frac{\left(\frac{1}{2}m_1 + \frac{1}{2}m_2\right) g}{\left(z_{3,0} - h_{\mathrm{SO}}\right)^2} \arctan\left(\varphi_{1,0}\right). \tag{19}$$

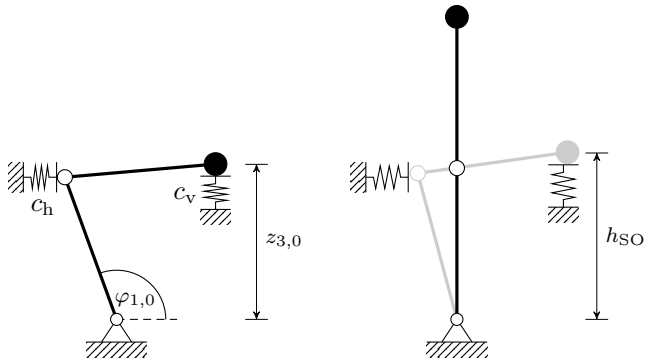

Fig. 2. *Left*: Model in sitting position; *Right*: Model in Seat-Off position (gray) and standing position (black)

3. JOINT TORQUE ESTIMATION

This sections describes the joint torque estimation based on inverse dynamics and measuring of the ground reaction forces. These are the classic approaches to estimate the joint torque for an active knee orthosis and will be used as a reference for the new approach described in the next section.

3.1 Inverse Dynamics

The formula to compute the input $\mathbf{u}$ from the measured joint angles can easily be derived from (10):

$$\mathbf{u} = {\mathbf{F}_{\mathrm{u}}}^{-1} \Big[\mathbf{M}(\mathbf{q})\ddot{\mathbf{q}} + \mathbf{K}(\mathbf{q}, \dot{\mathbf{q}}) - \mathbf{F}_f(\mathbf{q}, \dot{\mathbf{q}}) \mathbf{f}_{\mathrm{Seat}} \Big]. \tag{20}$$

Obviously, the first and second derivatives of the joint angles $\mathbf{q}$ are required to compute the joint torques $\mathbf{u}$. Typically, only the joint angles can be measured directly; therefore, the derivatives have to be computed numerically. With the joint angle signal usually being noisy, it is a challenging task to derive a feasible signal for the joint torques. Moreover, the seat forces $\mathbf{f}_{\mathrm{Seat}}$ or at least the joint angles $\varphi_{i,0}$ in sitting position are required, too. These could be estimated with a situation recognition algorithm, for example.

3.2 Ground Reaction Forces

The ground reaction forces and the center of pressure can be determined if two or more force sensors are attached to the shoe sole. If the ankle angle is measured, too, it is possible to compute the joint torques with a straight forward approach. For a proper estimation of the joint forces and torques, it is necessary to measure the shear forces $F_{i,\mathrm{x}}$ in longitudinal direction of the foot in addition to the normal forces $F_{i,\mathrm{z}}$. The two (or more) measured ground reaction forces can be summarized in the center of pressure as seen in Fig. 3:

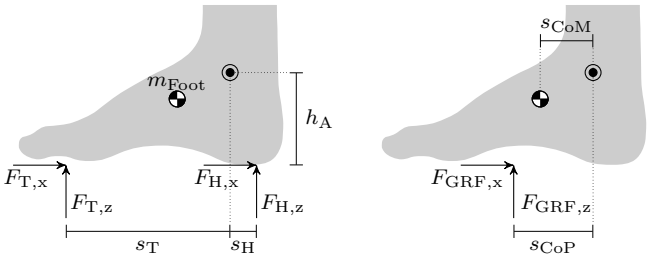

Fig. 3. Ground Reaction Forces and Center of Pressure

$$F_{\mathrm{GRF,x}} = F_{\mathrm{T,x}} + F_{\mathrm{H,x}} \tag{21}$$

$$F_{\mathrm{GRF,z}} = F_{\mathrm{T,z}} + F_{\mathrm{H,z}} \tag{22}$$

$$s_{\mathrm{CoP}} = \left(F_{\mathrm{T,z}}\, s_{\mathrm{T}} - F_{\mathrm{H,z}}\, s_{\mathrm{H}}\right) / \left(F_{\mathrm{T,z}} + F_{\mathrm{H,z}}\right). \tag{23}$$

With the simplifications of section 2.1 and the free body diagram depicted in Fig. 4, the ankle joint forces and torques can be computed

$$F_{\mathrm{A,x}} = F_{\mathrm{CoP,x}} \tag{24}$$

$$F_{\mathrm{A,z}} = F_{\mathrm{CoP,z}} - m_{\mathrm{Foot}}\, g \tag{25}$$

$$M_{\mathrm{A}} = F_{\mathrm{CoP,x}}\, h_{\mathrm{A}} - F_{\mathrm{CoP,z}}\, s_{\mathrm{CoP}} + m_{\mathrm{Foot}}\, g\, s_{\mathrm{CoM}}. \tag{26}$$

With these values, the ankle angle φ_1, the mass m_1, and the length l_1 of the shank, the knee torque can be determined

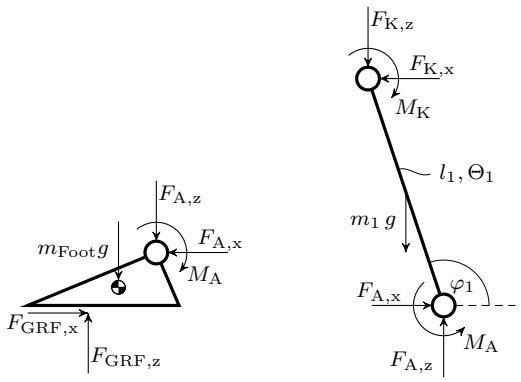

Fig. 4. Free Body Diagram of the human lower extremity *Left:* Foot, *Right:* Shank

$$M_{\mathrm{K}} = M_{\mathrm{A}} + F_{\mathrm{A,x}}\, l_1 \sin(\varphi_1) - F_{\mathrm{A,z}}\, l_1 \cos(\varphi_1) + \ldots \\ \ldots + m_1 g \tfrac{l_1}{2} \cos(\varphi_1) - \Theta_1^{(\mathrm{K})} \ddot{\varphi}_{\mathrm{A}}, \tag{27}$$

with $\Theta_1^{(\mathrm{K})}$ being the moment of inertia of the shank with respect to the knee joint. Note that the seat forces are not required in order to determine the knee torque though the ankle angular acceleration $\ddot{\varphi}_1$ is. However, this term can be neglected since the torque of inertia is small compared to the other forces (see Fig. 7.) Therefore, no derivation of the angular signal needs to be computed.

4. OBSERVER BASED JOINT TORQUE ESTIMATION

As seen in the previous section, the correct estimation of the joint torques strongly depends on the accurate measurement of the ground reaction forces. A mismeasurement not only affects the forces themselves, but also the center of pressure as seen in (23). Both signals have a considerable influence on the estimated joint torques. However, some problems arise when using force sensors in the shoe sole: While the distance between the two (or more) force sensors is known, the exact distances between the sensors and the ankle joint, s_{T} and s_{H}, might be uncertain. The same applies for the vertical distance h_{A} between the ankle joint and the shoe sole. Moreover, the foot might move within the shoe and therefore change these values, too.

That means the computed joint torques are flawed or disturbed:

$$\tilde{\mathbf{u}} = \mathbf{u} + \mathbf{z}. \tag{28}$$

An observer can estimate these disturbances $\mathbf{z}$ and the original signal can be restored if the estimated disturbances are substracted from the computed joint torques.

$$\hat{\mathbf{u}} = \tilde{\mathbf{u}} - \hat{\mathbf{z}} = \mathbf{u} + \mathbf{z} - \hat{\mathbf{z}}. \tag{29}$$

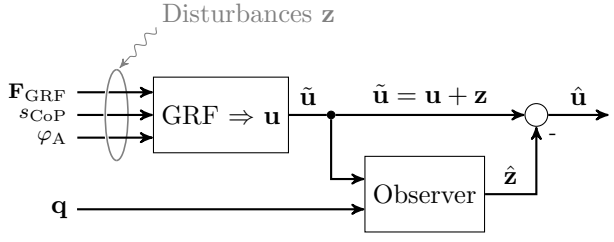

Fig. 5. Observer based joint torque estimation

The disturbances $\mathbf{z}$ can be considered as an additional input to the model specified in section 2.1. The extended state space description is as follows:

$$\dot{\mathbf{x}} = \mathbf{f}(\mathbf{x}) + \mathbf{g}_{\mathrm{u}}(\mathbf{x})\mathbf{u} + \mathbf{g}_{\mathrm{f}}(\mathbf{x})\mathbf{f}_{\mathrm{Seat}} + \mathbf{e}(\mathbf{x})\mathbf{z}, \tag{30}$$

and since the disturbances act on the control input,

$$\mathbf{e}(\mathbf{x}) = \mathbf{g}_{\mathrm{u}}(\mathbf{x}). \tag{31}$$

It is assumed, that the disturbances are piecewise constant, therefore:

$$\begin{aligned} \dot{\mathbf{x}}_{\mathrm{z}} &= \mathbf{0} \\ \mathbf{z} &= \mathbf{x}_{\mathrm{z}}. \end{aligned} \tag{32}$$

4.1 Extended Kalman Filter

An extended state space description can be derived by combining (30), (31) and (32):

$$\underbrace{\begin{bmatrix} \dot{\mathbf{x}} \\ \dot{\mathbf{x}}_{\mathrm{z}} \end{bmatrix}}_{\dot{\mathbf{x}}_{\mathrm{g}}} = \underbrace{\begin{bmatrix} \mathbf{f}(\mathbf{x}) + \mathbf{g}_{\mathrm{u}}(\mathbf{x})\mathbf{x}_{\mathrm{z}} \\ \mathbf{0} \end{bmatrix}}_{\mathbf{f}_{\mathrm{g}}(\mathbf{x}_{\mathrm{g}})} + \underbrace{\begin{bmatrix} \mathbf{g}_{\mathrm{u}}(\mathbf{x}) \\ \mathbf{0} \end{bmatrix}}_{\mathbf{g}_{\mathrm{g,u}}(\mathbf{x}_{\mathrm{g}})} \mathbf{u} + \underbrace{\begin{bmatrix} \mathbf{g}_{\mathrm{f}}(\mathbf{x}) \\ \mathbf{0} \end{bmatrix}}_{\mathbf{g}_{\mathrm{g,f}}(\mathbf{x}_{\mathrm{g}})} \mathbf{f}_{\mathrm{Seat}}$$

$$\mathbf{q} = \underbrace{\begin{bmatrix} \mathbf{h}(\mathbf{x}) \\ 0 \end{bmatrix}}_{\mathbf{h}_{\mathrm{g,q}}(\mathbf{x}_{\mathrm{g}})} \qquad \mathbf{z} = \underbrace{\begin{bmatrix} 0 \\ \mathbf{I}\,\mathbf{x}_{\mathrm{z}} \end{bmatrix}}_{\mathbf{h}_{\mathrm{g,z}}(\mathbf{x}_{\mathrm{g}})} \tag{33}$$

An extended kalman filter (EKF) is used for estimating the states $\mathbf{x}_{\mathrm{g}}$. The estimation equation is as follows:

$$\dot{\hat{\mathbf{x}}}_{\mathrm{g}} = \mathbf{f}(\hat{\mathbf{x}}_{\mathrm{g}}) + \mathbf{g}_{\mathrm{g,u}}\tilde{\mathbf{u}} + \mathbf{g}_{\mathrm{f,u}}\mathbf{f}_{\mathrm{Seat}} + \mathbf{L}(t)\big(\mathbf{q} - \mathbf{h}_{\mathrm{g,q}}(\hat{\mathbf{x}}_{\mathrm{g}})\big) \tag{34}$$

The observer matrix $\mathbf{L}$ is timevariant and derived by the well known Riccati equation:

$$\begin{aligned} \mathbf{L}(t) &= \mathbf{P}(t)\mathbf{C}^{\mathrm{T}}(t)\mathbf{S}^{-1} \\ -\mathbf{Q} &= \mathbf{A}^{\mathrm{T}}(t)\mathbf{P}(t) + \mathbf{P}(t)\mathbf{A}(t) - \mathbf{P}(t)\mathbf{C}(t)\mathbf{S}^{-1}\mathbf{C}^{\mathrm{T}}(t)\mathbf{P}(t). \end{aligned} \tag{35}$$

The matrices $\mathbf{A}(t)$ and $\mathbf{C}(t)$ are linearizations of the plant and input vector fields:

$$\begin{aligned} \mathbf{A}(t) &= \left.\frac{\partial\left(\mathbf{f}_{\mathrm{g}} + \mathbf{g}_{\mathrm{g,f}}\mathbf{f}_{\mathrm{Seat}}\right)}{\partial \mathbf{x}_{\mathrm{g}}}\right|_{\hat{\mathbf{x}}(t)} \\ \mathbf{C}(t) &= \left.\frac{\partial \mathbf{g}_{\mathrm{g,u}}}{\partial \mathbf{x}_{\mathrm{g}}}\right|_{\hat{\mathbf{x}}(t)} \end{aligned} \tag{36}$$

and have to be computed online as well as the observer matrix $\mathbf{L}(t)$. Note that again, the seat forces are required for the computation of the joint torques.

5. SIMULATION RESULTS

5.1 Simulation Environment

The setup depicted in Fig. 6 is used for the evaluation of the three different approaches. In addition to the joint angles $\mathbf{q}$, the ground reaction forces and the center of pressure are also provided by the model as these signals will be measured in the real orthosis as well. These three signals are superimposed with white noise of different intensities to emulate noisy sensor signals. Additional signals can be imposed to simulate a movement of the foot in the shoe, for example. Furthermore, the shear

force component of the ground reaction forces can be suppressed.

To simplify matters, the three approaches will be named *GRF-estimator*, for the computation of the knee torque using ground reaction forces, *ID-estimator* for the computation of the knee torque using inverse dynamics and *OBS-estimator* for the new approach, respectively.

Due to noisy signals, it is necessary to filter the angles $\mathbf{q}$ before differentiating. Therefore, a third order state-variable filter with a cut-off frequency of 40 Hz was inserted before the ID-estimator.

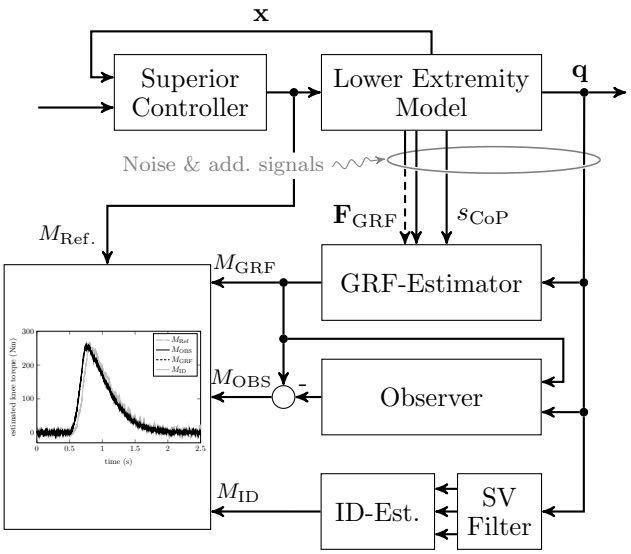

Fig. 6. Simulation Setup

As our orthosis enhances the strenght of the knee joint, only the knee torques will be discussed in the following section. However, all results apply for the ankle joint as well.

The parameters for the simulation are chosen according to the factors presented in Nigg and Herzog (1995), based on a 100 kg subject. These values are referenced as "Ref." in table 1. Furthermore, the parameters were randomly modified by up to $\pm$ 20 % and referenced as "Mod.". These modified parameters are used for the computation of the joint torques and simulate a difference between the model (20), (27), or (34) and the system (15) with the reference parameters, which is always present in reality.

Table 1. Parameters

	Ref.	Mod.	Unit		Ref.	Mod.	Unit
m_1	4.0	4.36	kg	d_1	0	0	$\frac{\mathrm{N\,m\,s}}{\mathrm{rad}}$
m_2	10.3	11.35	kg	d_2	0	0	$\frac{\mathrm{N\,m\,s}}{\mathrm{rad}}$
m_3	35.7	32.5	kg	l_1	0.5	0.55	m
J_1	0.367	0.393	$\mathrm{kg\,m^2}$	l_2	0.5	0.59	m
J_2	0.551	0.585	$\mathrm{kg\,m^2}$	$\varphi_{1,0}$	100	97.5	°
g	9.81	9.81	$\mathrm{m/s^2}$	$\varphi_{2,0}$	5	4.76	°

The observer parameters are chosen as follows:

$$\mathbf{Q} = \mathrm{diag}\left[1^0\ 1^0\ 1^0\ 1^0\ 1^{13}\ 1^{13}\right], \qquad \mathbf{S} = \mathrm{diag}\left[1^2\ 1^2\right].$$

5.2 Simulation Results

For the first plot it is assumed that no parameter deviation between the system and the models in the joint torque estimators is present. That means the paramters "Ref." are used for the system as well as for the models.

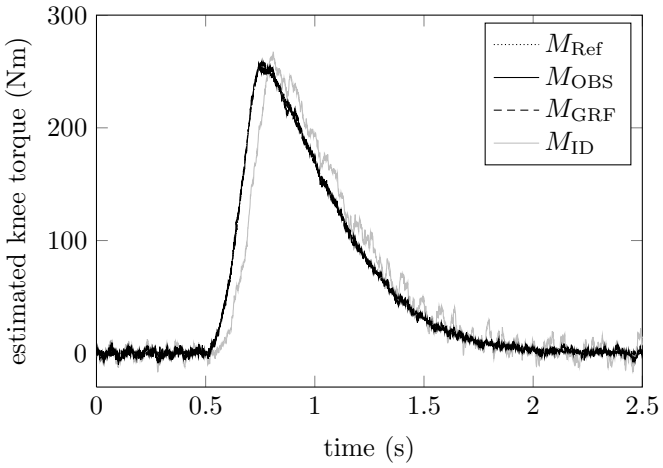

Fig. 7. Estimated knee torques; noisy signals

As expected, all three knee torque estimators produce excellent results if the parameters of the models match those of the reference. However, due to the filtering of the angular signals, a significant phase lag occurs with the ID-estimator. This signal is also noisier than the signals from the other two estimators. The noise could be reduced by decreasing the cut-off frequency of the state-variable filter, though this would further increase the phase lag.

The signal from the ID-estimator would not be adequately usable as an input for an active orthosis. Especially the phase lag is a major disadvantage since it would cause the additional torque at the knee joint to be asynchronous to the user's demand.

It can also be seen that the neglected torque of inertia in the GRF-estimator does not have any significant impact on the computed knee torque, as no deviation of the GRF-signal from the reference signal is visible.

So far, the results were based on the presumption that the measurement of all signals is only disturbed by zero mean noise and that the shear force component of the ground reaction forces could be measured. Now the modified parameters ("Mod.") will be used for the models, except for the initial angles $\varphi_{i,0}$, which are held at the reference values. Also, the shear force component will be removed from the ground reaction forces. For better illustration, no noise is implemented; however, the state-variable filter is still present, since it would be necessary with a noisy signal.

As expected, the signal from the GRF-estimator does now not match the reference signal as well as before. This is mainly due to the missing shear force component. The deviation of the signal *during* the Sit-to-Stand movement from the reference is not a problem for an active orthosis as this would only produce a slightly higher or lower support torque that the user could easily compensate. The bigger problem, however, is the non-zero estimate prior to

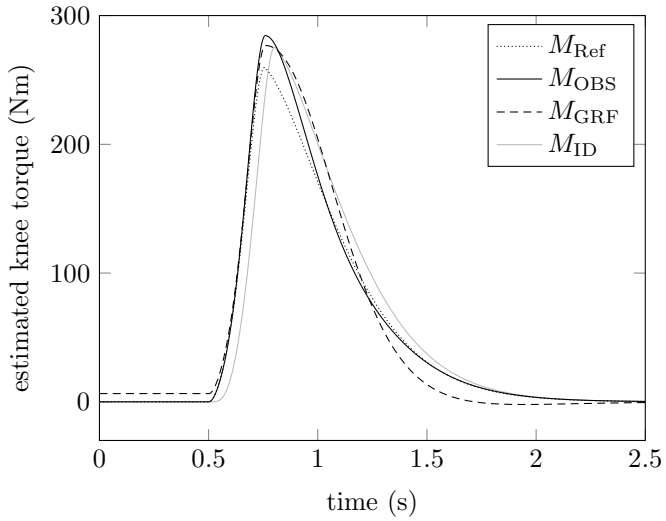

Fig. 8. Estimated knee torques; deviating parameters

the STS movement which would cause an uncomfortable and undesired additional torque at the knee joint during sitting.

The corrected signal from the OBS-estimator, though, has a higher deviation from the reference signal at the maximum but converges better to the reference signal thereafter, while the signal from the GRF-estimator deviates considerably. Moreover, the OBS-estimator produces zero torque during sitting since the missing shear force component is estimated as a disturbance and compensated.

To simulate a movement of the foot inside the shoe, a step signal of 20 mm is added to the center of pressure s_{CoP} after 1 s of simulation time.

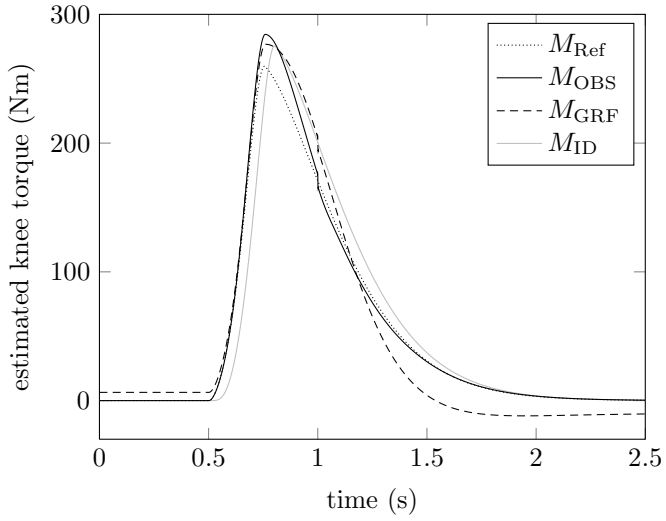

Fig. 9. Estimated knee torques; step of 20 mm in s_{CoP} at a simulation time of 1 s

The impact of the mismeasurement of the ground reaction forces can be seen at the end of the Sit-to-Stand movement. Here, the GRF-estimator produces a non-zero estimation of the knee torque, which is undesirable and might be uncomfortable or even painful for the user if used as an input for an active orthosis. The OBS-estimator, on the other hand, can compensate the mismeasurement and produces a zero torque estimate of the knee torque.

Finally, also the initial angles $\varphi_{i,0}$ are modified. It can be seen that all estimators produce a non-zero estimate prior to the STS transfer. However, the OBS estimator still has a zero torque estimate in the standing position.

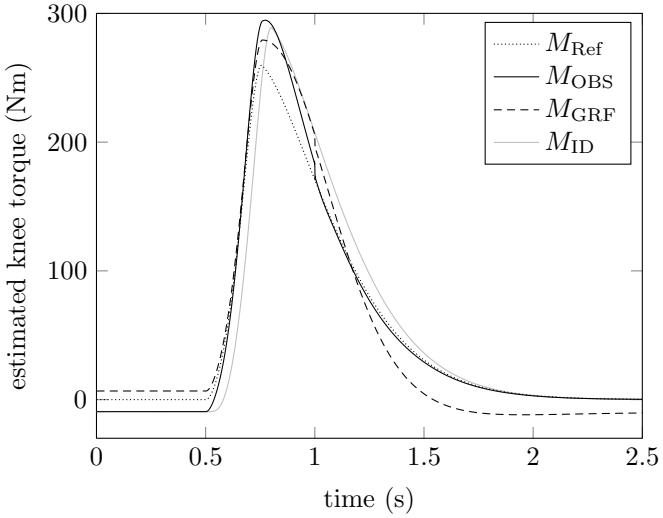

Fig. 10. Estimated knee torques; modified initial angles $\varphi_{i,0}$ and step of 20 mm in s_{CoP}

The simulation shows that an exact measurement of the initial angles in the sitting position is necessary if the OBS-estimator is chosen. However, a zero torque support in the standing position can be achieved even if the measurement of the ground reaction forces is disturbed.

REFERENCES

Fleischer, C. and Hommel, G. (2006). Torque control of an exoskeletal knee with EMG signals. In *Proceedings of the Joint Conf. on Robotics: ISR 2006 and Robotik 2006*.

Hayashi, T., Kawamoto, H., and Sankai, Y. (2005). Control method of robot suit HAL working as operator's muscle using biological and dynamical information. In *IEEE/RSJ Int. Conf. on Intelligent Robots and Systems (IROS '05), 2005*, 3063–3068.

Isidori, A. (1995). *Nonlinear Control Systems*. Springer-Verlag New York, Inc., Secaucus, NJ, USA, 3rd edition.

Kazerooni, H., Racine, J.L., Huang, L., and Steger, R. (2005). On the control of the Berkeley lower extremity exoskeleton (BLEEX). In *Proceedings of the 2005 IEEE Int. Conf. on Robotics and Automation (ICRA '05) 2005*, 4353–4360.

Kong, K. and Tomizuka, M. (2009). Control of exoskeletons inspired by fictitious gain in human model. *IEEE/ASME Transactions on Mechatronics*, 14(6), 689–698.

Nigg, B. and Herzog, W. (1995). *Biomechanics of the musculo-skeletal system*. J. Wiley, Chichester; New York.

Pratt, J., Krupp, B., Morse, C., and Collins, S. (2004). The RoboKnee: an exoskeleton for enhancing strength and endurance during walking. In *Proceedings of the IEEE Int. Conf. on Robotics and Automation (ICRA '04), 2004*, volume 3, 2430–2435.